Coastal Dynamics 2017
Paper No. 210

CLIMATE CHANGE-DRIVEN CLIFF AND BEACH EVOLUTION AT DECADAL TO CENTENNIAL TIME SCALES

Li Erikson[1], Andrea O'Neill[1], Patrick Barnard[1], Sean Vitousek[2], and Patrick Limber[1]

Abstract

Here we develop a computationally efficient method that evolves cross-shore profiles of sand beaches with or without cliffs along natural and urban coastal environments and across expansive geographic areas at decadal to centennial time-scales driven by 21st century climate change projections. The model requires projected sea level rise rates, extrema of nearshore wave conditions, bluff recession and shoreline change rates, and cross-shore profiles representing present-day conditions. The model is applied to the ~470-km long coast of the Southern California Bight, USA, using recently available projected nearshore waves and bluff recession and shoreline change rates. The results indicate that eroded cliff material, from unarmored cliffs, contribute 11% to 26% to the total sediment budget. Historical beach nourishment rates will need to increase by more than 30% for a 0.25 m sea level rise (~2044) and by at least 75% by the year 2100 for a 1 m sea level rise, if evolution of the shoreline is to keep pace with rising sea levels.

Key words: profile evolution, long-term shoreline change, cliffs, sandy coastlines, climate change

1. Introduction

The evolution of sand and cliff-backed shores at decadal to centennial scales is the result of processes operating over short (e.g., tides, storms), medium (e.g., seasonal/annual), and long-term (e.g., sea-level rise (SLR), regional sediment supply) time-scales. Predictions of long-term coastal evolution are notoriously difficult considering the general lack of long-term historical coastal change data and the multitude of physical processes that drives change. Coastal change is further complicated by infrastructure and anthropogenic activities such as damming, sand mining, dredging, and beach nourishment in highly urban areas (e.g., Stive et al., 2002). Yet predictions of coastal evolution are essential for the effective management, planning, and projection of coastal hazards in anticipation of climate change (Ranasinghe and Stive, 2009).

Physics-based models (e.g. Delft3D (Roelvink and Van Banning, 1995), XBeach (Roelvink et al., 2010), Mike21 (Warren and Bach, 1992, Kaergaard and Fredsoe, 2013), and ROMS (Warner et al., 2010)) compute hydrodynamics, waves, morphology, sediment transport, and other relevant physics responsible for coastal morphologic change, but are typically limited to small-scale, short-term (days to months) simulations due to lengthy computation times. To describe long-term behavior, both physical factors (e.g., SLR, changing wave climate and water level extremes) and morphodynamic conditions (e.g., aeolian transport, tectonics, beach nourishment) need to be taken into account.

Recent advances in long-term shoreline change modeling are able to efficiently project >100-year long time-series with short computational times (<1 week) and incorporate physics, historical trends, and changes in nearshore wave and water level conditions. Two such models were developed for the Southern California (USA) coast: one for coastal cliff retreat (Limber et al., 2015) and another for erosion and accretion of sandy shorelines (Vitousek et al., 2017). The coastal cliff retreat model (Limber et al., 2015) employs one soft rock (loosely consolidated sediment deposits) and one hard rock (indurated lithologies such as sandstone or granite) process-based model (Trenhaile, 2011; Walkden and Hall, 2005), and a variable beach slope that changes with volumetric loss of cliff material and allows for variations in maximum runup of time-varying offshore waves. The second model, referred to as the Coastal One-line Assimilated Simulation Tool, CoSMoS-COAST (Vitousek et al., 2017), computes long-term projections of sandy shorelines. The CoSMoS-COAST model incorporates historical trend analysis and improvements to three process-based models that compute both long- and cross-shore transport along shore-normal transects. Both the cliff and sandy shore models have been applied to the Southern California Bight using

time-varying projected wave conditions for the 21st century (Hegermiller et al. 2016) in combination with a range of SLR rates. The results consist of projected shoreline positions defined as the top of the cliff or mean-high-water (MHW) line for the cliff and sandy shore models, respectively.

Although it is relatively straight-forward and reasonable to assume that the slope of a cliff face remains constant as the top of the cliff recedes, the shape of sandy shore profiles can vary significantly from their initial state depending on existing or expected infrastructure, seasonality, vegetation, and changing wave conditions. In particular, a change in wave conditions will alter the active beach width (ABW) and thus the extent over which a shore-normal profile erodes or accretes. The ABW extends from the offshore end of bathymetric change and landward up to where tides, waves, and storm surge reach and actively alter the beach. For example, an increase in extreme wave heights will cause waves to break farther offshore and runup farther onshore. In contrast, decreases in wave heights will result in breaking closer to shore and shorter runup lengths, effectively decreasing the distance over which a profile is expected to change. Variations of the extents to which shore-normal coastal profiles are estimated to change has implications on volume calculations and modeling efforts that aim to include shoreline change and flooding.

In this study, a profile evolution model that efficiently evolves shore-normal profiles of sandy coastlines with or without cliffs along natural and urban coastal environments across expansive geographic areas and at decadal to centennial time-scales is presented. Required inputs include an initial profile (assumed to be at equilibrium, see Section 3.1), cliff recession rates provided here from the Limber model, changes in MHW positions provided here from the Vitousek model (or other point defining a shoreline), SLR, and nearshore wave conditions. An overview of the profile types considered and the methodology used to evolve the profiles are presented in Sections 2 and 3. Using results of the cliff (Limber et al 2015) and sandy shoreline (CoSMoS-COAST, Vitousek et al. 2017) models developed for the Coastal Storm Modeling System (CoSMoS: Barnard et al., 2014), the profile evolution model is applied to the Southern California Bight, USA. Select profiles within the study area that have been evolved in response to SLR and 21st century storms are presented in Section 4 as are estimates of total changes in sediment volumes at discrete littoral cells within the Bight and for entire region, assuming two end-member cases of a sediment-starved system and one with ample sediment availability.

2. Profile Types Considered

The profile evolution model considers three possible profile types:

1) Cliff with or without a narrow fronting beach. Recession (ΔR) is defined at the top of the cliff.

2) Sandy shore, with or without infrastructure or vegetation. Change is defined as landward (erosion, $+\Delta S$) or seaward (accretion, $-\Delta S$) migration of the MHW position.

3) Cliff-backed sandy beach (combination of (1) and (2)). ΔR and ΔS both apply.

Each profile extends from the depth of closure to the 10 m inland topographic contour. The depth of closure is the seaward limit at which seasonal bed level changes become smaller than survey accuracy (Birkemeier, 1985), here conservatively estimated to range from 15-20 m based on the local wave climate and the limited sites with repeated bathymetric profile data. Profiles obtained as part of this study and used in the example application at the end of this manuscript were extracted from a seamless 2-m bare-earth digital elevation model (DEM) compiled from the most recent airborne lidar and multi-beam bathymetry primarily collected during the fall months (Danielson et al., 2016; Thatcher et al., 2016). To obtain the profiles, 2-m equally-spaced points along approximate shore-normal transects were first generated and then nearest-neighbor elevations (referenced to the North American Vertical Datum of 1988, NAVD88) were extracted.

3. Profile Evolution Models

The profile evolution model presented here is based on the equilibrium beach profile concept and conserves volume along a given profile, except in cases where infrastructure exists or the sub-aerial or sub-

aqueous bed slopes exceed generally accepted stable slopes after placement of eroded volumes. The subsequent sections provide details on the sandy shore and cliff profile evolution models (Figure 1); for profiles with beaches fronting cliffs, a combination of the two evolution approaches is used.

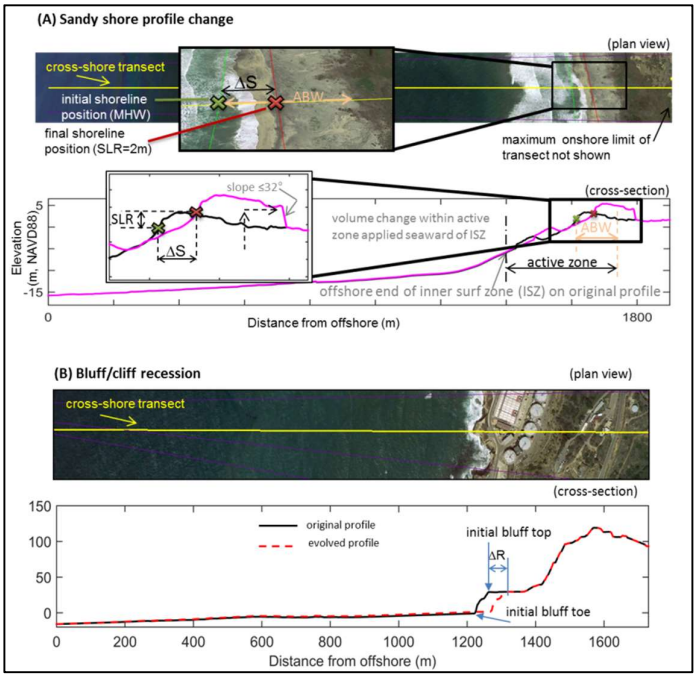

Figure 1. Two main profile types considered in the profile evolution model. (A) Schematic of key parameters used in the evolution of soft (sand and gravel) beaches. The example shows a landward translation of the original profile (black) to the final profile (pink). Changes in the shoreline position (ΔS) are indicated as the migration from the green to red X. The new shoreline position is found as the intersection of the inner surf zone slope with the original profile landward of the initial MHW line (red X). The remaining profile is merged with the original using an angle of 32° (angle of repose for dry sand (Bird, 2000)). (B) Schematic of key parameters used in the evolution of cliff profiles. The section defining the initial bluff toe and top of the cliff are translated landward by ΔR. The foreshore and hinterland portions of the translated profile are linearly interpolated to merge with the original profile.

3.1. *Sandy shore profile evolution*

The sandy shore profile is assumed to be in 'dynamic' equilibrium (NRC 1987; Pilkey at al., 1993; Larson and Kraus, 1989) such that a profile undergoes time-dependent adjustments about an average shape based on factors such as sediment type and supply, prevailing wave and wind conditions, and sea level. Here we represent the average beach shape by the initial (measured) profile. The initial measured profiles do not account for seasonal and inter-seasonal variability but are primarily representative of fall conditions which corresponds to when the majority of the lidar data was collected (see Section 2). Although only limited temporal data exist, fall surveys from 2005 through 2016 in the north-central portion of the study region show only small deviations in areas away from river mouths and submarine canyons (pers. comm. Dan Hoover, 2017), suggesting that an equilibrium profile is a reasonable assumption.

Dynamic equilibrium profiles differ from idealized geometric equilibrium profiles that are assumed to maintain a short and steep limb near the shore and elongated flat limb offshore (Dean, 1991). Both the geometric and dynamic equilibrium concepts are supported by copious amounts of research that indicate that, despite the inherent variability of nearshore processes, coastal systems tend toward equilibrium configurations with defined geometries (Fagherazzi et al., 2003; Fitzgerald et al., 2008).

The equilibrium profile concept is a staple in the well-known 'Bruun Rule' (Bruun, 1954, 1962), one of the first and simplest profile translation models. The Bruun Rule relates shoreline retreat to the product of SLR and the ratio of the horizontal to vertical dimensions of the active profile. The profile is

translated landward and upward without a change in form; eroded sand from the upper portions of the profile is deposited seaward to raise the seaward active part of the profile by SLR. This 'Rule' has served as a basis for more than 5 decades of innumerable studies that aim to estimate long-term coastal profile change. In its original form, the Bruun Rule only allowed for seaward net sediment transport, but since that time many field and laboratory investigations have established that build-up and translation of the sub-aerial portion of the active zone also occurs in conjunction with SLR due to for example aeolian transport and overwash (Rosati et al., 2013; Larson et al., 2015; Davidson-Arnott, 2005; Cowell et al., 1995; Carter, 1988). Most long-term Bruun-based profile evolution models that account for onshore sediment transport either assume an intact dune system (e.g., Carter et al., 1988), some maximum berm height (e.g., Cowell et al., 1995), or schematized sand overwash volumes (e.g., Rosati et al., 2013).

The sandy shore profile evolution model developed for this study employs the concept of the horizontal and vertical translation of a profile in dynamic equilibrium, including relevant portions of the sub-aerial profile, whilst accounting for existing infrastructure (Figure 1A). The portion of the profile that undergoes translation extends from the seaward end of the inner surf zone (ISZ) to a sub-aerial point that estimates the location of active tide, wave, and storm surge effects or flood protection infrastructure.

The seaward end of the inner surf zone (ISZ) is used to define the offshore limit of profile translation and separate the erosion / accretion signal for conservation of sand volume. The inner surf zone is defined by the depth of incipient wave breaking estimated with,

$$h_b = \frac{H_b}{\gamma_b} \tag{1}$$

in which H_b is the wave height at incipient breaking, and γ_b is the breaker depth index. H_b is estimated with

$$H_b = \varphi_b H_o' \tag{2}$$

where φ_b is the breaker height index ($= 0.56\left(H_o'/1.56T_p^2\right)^{-1/5}$ with T_p = peak wave period, (Komar and Gughan 1973) and H_o' the un-refracted deep-water wave height. For mild inner surf zone slopes ($tan\beta \leq 0.09$, between water depths -0.2 m to 3 m at the shore), the breaker depth index is estimated with an empirically based relationship developed by Raubenheimer and Guza (1996) and for steeper slopes a relationship by Battjes (1974) is used,

$$\gamma_b = \begin{cases} 0.2 + 5.98 \cdot tan\beta & \dots for\ tan\beta \leq 0.09 \\ 1.062 + 0.137 \cdot log\left(tan\beta/\sqrt{H_o/L_o}\right) & \dots for\ tan\beta > 0.09 \end{cases} \tag{3}$$

where H_o is the back-calculated deep water wave height and L_o is the deep water wavelength. The landward limit (LLT) of the profile is defined by one of the following criteria, in the order listed:

- Active beach width, defined by vegetation lines digitized from aerial photography obtained in June/July 2015 and March 2016 (Google Earth). Vegetation lines were decipherable at 612 of the 4,802 profiles (13 %).
- Intersection of the inner surf zone slope with the original profile landward of the initial MHW line (similar in concept to the intersection of the submerged profile in the Bruun Rule, e.g., Rosati et al., 2013).
- Non-erodible line (NEL) defined by existing infrastructure identified from aerial images or available records.
- Regionally-averaged active beach width (= 93 m ± 76 m, at 612 profiles within the Southern California Bight, as described in the first bullet above).

Following translation by ΔS in the horizontal and by SLR in the vertical of the profile sub-section between ISZ and LLT, the remaining portion of the profile was merged with the original profile assuming a 32° angle of repose for dry sand (Bird 2000) at the landward end, and by simple linear fitting at the seaward end. The change in volume landward of the seaward end of ISZ was computed and distributed (or removed) across the submerged portion of the profile seaward of the surf zone limit, tapering off to zero or near zero at the depth of closure. A flowchart of the methodology is shown in Figure 2.

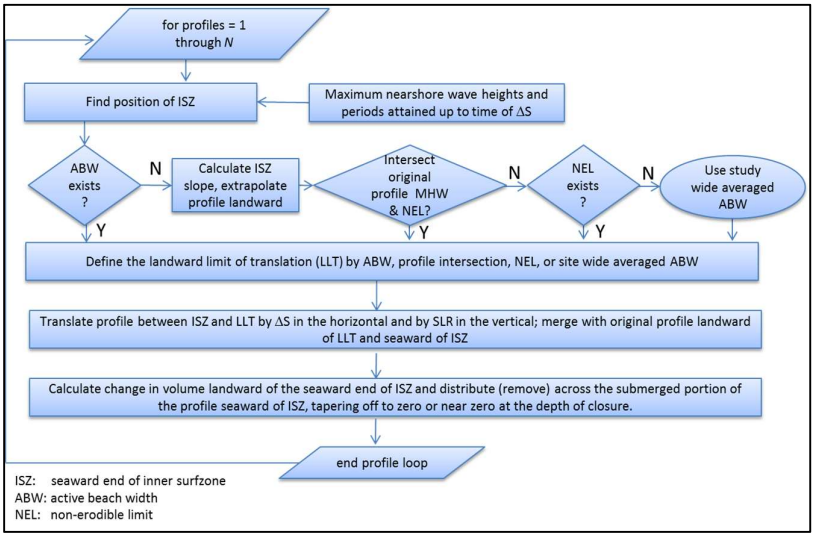

Figure 2. Flow chart summarizing the method used to evolve sandy shore profiles.

3.2. *Cliff profile evolution*

For profiles where the cliff toe and top had not yet been identified *a priori* via the approach of Limber et al. (2015), piecewise linear segments were fit to the profile and the point of inflection from near vertical to near horizontal was identified as the cliff top. The cliff toe was located using a similar approach based on changes in slope but limited to searching the profile seaward of the identified cliff top location. Profile elevations between the cliff toe and top were consequently translated by ΔR and the fronting beach linearly extrapolated from the original cliff toe position to the intersection with the translated cliff face. The original foreshore slope immediately fronting the original cliff face position was maintained in the extrapolation. The volume (per unit length of beach or area in case of these one-line models) eroded was then calculated and dispersed between the new toe position and depth of closure so that the added height at the offshore end coincident with the depth of closure was zero. In this way, volume was conserved across the profile (Young et al., 2014). An exception to this was applied for cases where the distributed material exceeds the angle of repose; for those cases, a maximum added sediment depth of SLR was applied.

4. Application to the Southern California Bight

ΔS and ΔR were computed with the CoSMoS-COAST shoreline change (Vitousek et al., 2017) and cliff retreat (Limber et al., 2015) models using a 100-yr long time-series of projected nearshore wave conditions (Hegermiller et al., 2016; Figure 3A) and the SLR curve of the National Research Council (NRC, 2012; Figure 3B). The NRC SLR curve reaches 93.1 cm above year 2000 levels by 2100. To evaluate ΔS and ΔR associated with higher rates of SLR, the cliff and shoreline change models were additionally run for the same time period using the same wave conditions, but with steeper SLR curves reaching values greater than 1 m by 2100. A total of 9 sea-level rise scenarios, ranging from 0.25 m to 2 m at 0.25-m increments and an additional 5 m scenario, were simulated for 2,017 profiles consisting of cliffs and 4,011 profiles consisting of sandy beaches backed by various environments. Both ΔS and ΔR were applied at 1,660 profiles (Figure 4).

All profiles were evolved for each of the nine SLR scenarios. Maximum wave heights and associated wave periods at the offshore ends of each of the profiles were used to compute the location of the inner surf zone (Eqs. 1-3). Maximum nearshore significant wave heights (H_s) and associated peak wave periods (T_p) during the relevant time periods at all of the transect points (including those that are affected by wave shadowing of offshore islands) range from 1 m to 5.9 m and 3.5 s to 20 s, respectively.

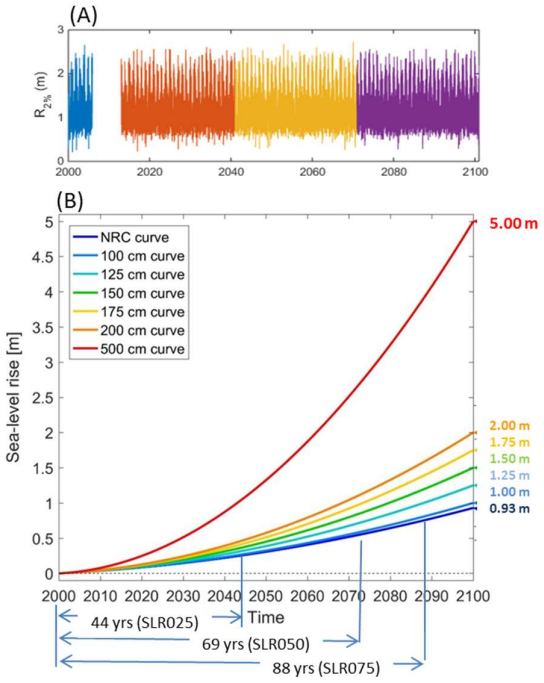

Figure 3. Wave and sea-level rise time-series used in the model. (A) Example time-series of Bight-wide averaged wave runup (a combination of wave height and period using the analytical equation of Stockdon et al. 2006 and an average foreshore slope of 0.03). (B) The nine sea-level rise curves used in the cliff recession (Limber et al., 2015) and CoSMoS-COAST (Vitousek et al., 2017) shoreline change models for Southern California (the blue 0.93 m curve applies to three SLRs <1 m). Figure modified from Vitousek et al., 2017.

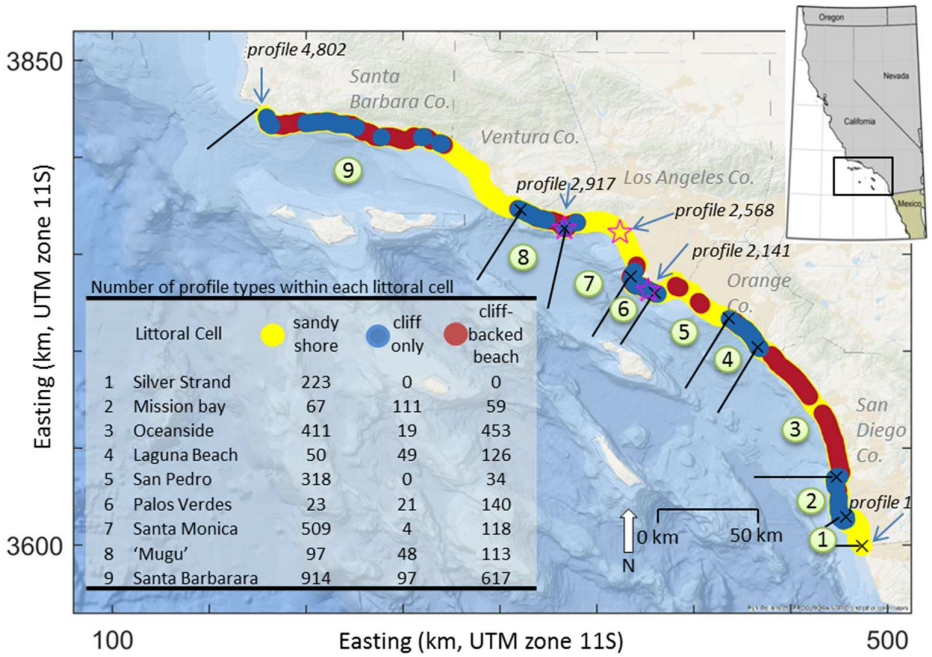

Figure 4. Map showing Southern California study area, littoral cells, locations of long-term evolved profiles, and the back-beach type at each transect.

4.1. *Decadal to centennial scale profile evolution*

Examples of cliff, sandy shore, and cliff-backed sandy shore profiles evolved for the 0.5, 1, 1.5, 2.0, and 5.0 m SLR scenarios are shown in Figure 5. Profile 2917 (Figure 5A) shows displacement of the cliff top and toe at a rate of approximately 10 m of cliff recession per half-meter rise in sea level. The slope of the cliff face and foreshore beach was maintained and material eroded was distributed across the shore resulting in a raised seabed.

The sandy shore profile at 2603 (Figure 5B) exhibits erosion ranging from 12.9 m to 129.7 m for the 0.50 m to 5.0 m SLR scenarios. The raised portions of the profiles represent landward transport of eroded sediment removed from the profile seaward of the inner surf zone (e.g., 5.0 m SLR scenario in Figure 5B). In the case of the example sandy shore profile 2603, a non-erodible structure was included at the abutting road located approximately 240 m landward of the initial MHW point. The rather wide (albeit flat) beach easily accommodates translation of the profile up to the 2 m SLR scenario. For the 5 m SLR scenario, the sand berm appears elevated and truncated at the non-erodible line (back slope is set at 32°, angle of repose for medium sized dry sand). In situations such as these in highly urban environments, the berm can be considered the result of beach management practices that aim to maintain access whilst protecting hinterland infrastructure from flooding.

The final example profile is that of a cliff-backed beach where both results from the cliff and sandy shore shoreline change models exist (Figure 5C). The cliff face (top to toe) recedes at a rate of approximately 3 m to 5 m per half meter of SLR. The rate is substantially lower than the rate noted for the similarly high cliff at profile 2917, likely a reflection of the fronting beach mitigating wave impacts to the toe of the cliff. The change in MHW position as simulated with the CoSMoS-COAST model indicates a maximum retreat of 19.0 m reached by the 1.0 m SLR scenario. The maximum retreat is a reflection of the initial position of the cliff toe. Beyond this point, the cliff recession model was deemed relevant over the CoSMoS-COAST beach change model.

4.2. *Volumetric sediment change with respect to SLR*

Two separate sets of evolved profiles were used to compute volumetric sediment changes with respect to SLR; the first set assumed a starved sediment system (cliff sediment was removed and bed levels were not raised) and the second, a system with ample sediment supply for which eroded cliff material stayed within the system and offshore sediment was allowed to transport landward. Volumetric changes at individual transects, dV^P (units of m^3/m), were estimated by calculating areas between evolved and originating profiles and multiplying and normalizing these by the alongshore distance, l_a, so that,

$$\mathrm{dV^P} = (\mathrm{dA} \cdot \mathrm{l_a})/\mathrm{l_a} \tag{4}$$

with

$$A = \int_0^{lc} [\, z^{SLR}(x) - z^{000}(x)]dx \tag{5}$$

where l_c is the cross-shore distance and z^{SLR} and z^{000} are profile elevations for the particular SLR of interest and the 0 m SLR reference level, respectively.

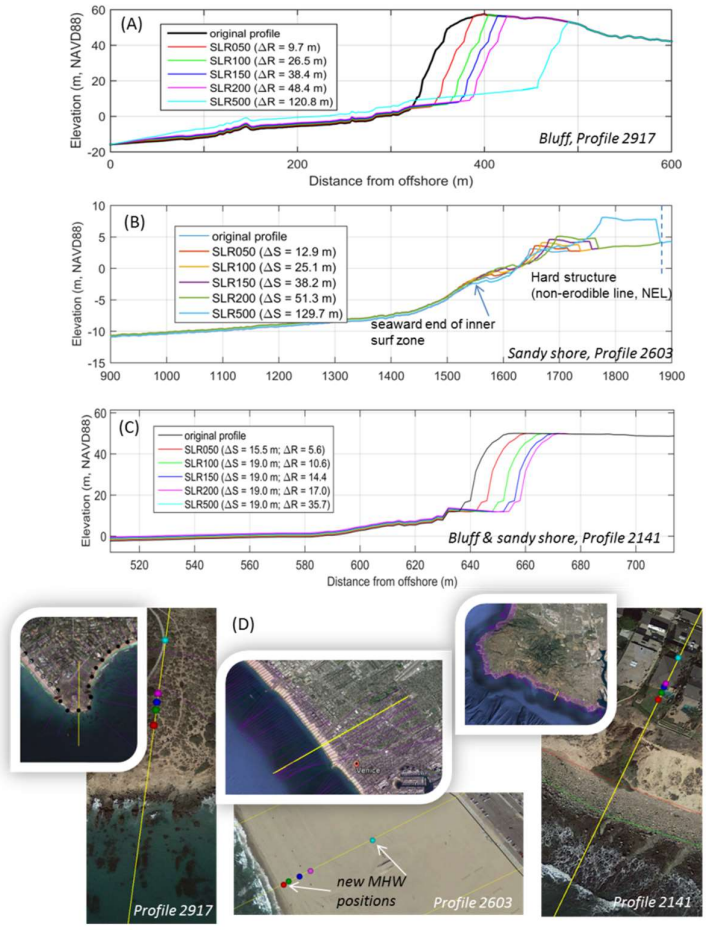

Figure 5. Example evolutions of the three profile types considered. (A) Cliff, (B) sandy shore, (C) cliff-backed sandy shore. (D) Aerial images and locations of the example profiles (Google Earth imagery, 2016). The plotted half meter SLR scenarios roughly represent the year 2070 for the 0.5 m SLR rise (SLR050) and the year 2100 for the remaining SLR scenarios.

For the end-member case of a starved sediment system, all profiles undergo a loss of material (Figure 6A,B), due to increased erosion with increasing SLR. Extrema are evident throughout the Bight, but most notably at profiles 296, 536, 561, 1145, 1410, 2316, 2846, 4024, and 4524 (Figure 6A), all of which are backed by high (>20 m) cliffs. The ranges of extreme volume change increases with increasing SLR (denoted as red plus signs in Figure 6B) as does the separation between the first and third quantiles (boxes in Figure 6B).

To assess rates of change throughout the Bight and at nine littoral cells (Flick, 1993) within the Bight, the profile area change data were summed up and normalized by the number of years for each SLR simulation,

$$\frac{\Delta V}{\Delta t} = \frac{\sum_{P=1}^{P=N}(dA^P \cdot l_a^P)}{\sum_{P=1}^{P=N} l_a^P} \times \frac{1}{Nyrs} \quad (6)$$

where N is the total number of profiles, the superscript P denotes profile number, and $Nyrs$ equals 100 for SLR scenarios ≥1 m and 44, 69, and 88 years for the 0.25 m, 0.50 m, and 0.75 m SLR scenarios respectively. A constant value of l_a = 100m was used in all calculations since transects are spaced approximately 100 m apart in the alongshore direction.

Results show a projected erosion rate of -2.9 m^3/m/yr for the 0.25 m SLR across the Bight (Figure 6C). This rate is commensurate with a sediment budget by Patch and Griggs (P&G, 2007), which suggests

a net reduction rate of -1.6 $m^3/m/yr$ (= $-7.6 \cdot 10^5$ m^3/yr from Table ii in P&G, divided by an approximate shoreline distance of 470,000 m). For SLRs greater than 0.25 m, the rates are projected to consistently increase up to -6.2 $m^3/m/yr$ and -12.3 $m^3/m/yr$ for the 2 m and 5 m SLRs, respectively. The predicted sediment loss exceeds recent historical nourishment rates (~2.18 $m^3/m/yr$, P&G, 2007) by 31%, 36%, 59%, and 74% for the 0.25 m, 0.50 m, 0.75 m, and 1.0 m SLR scenarios.

Erosion rates for the 'starved-sediment' scenario are fairly uniformly distributed between littoral cells (Figure 6D). The lowest rates are along the littoral cell here named 'Mugu' (-1.2 $m^3/m/yr$ to -7.9 $m^3/m/yr$ for the 0.25 m to 5 m SLR scenarios). The highest rates, -3.2 $m^3/m/yr$ to -20.3 $m^3/m/yr$ for the 0.25m and 5m SLR scenarios, are in the Palos Verdes littoral cell which is primarily lined with cliff-backed beaches (78%, 140 out of 180 profiles, Figure 4).

For the other end-member case where eroded cliff material is distributed across the beach and landward transport of sediment by, for example, overwash and aeolian transport, is estimated by raising and translating the active portion of the profile, the model projects a bight-wide erosion rate of -1.9 $m^3/m/yr$ for the 0.25 m SLR (Figure 7C). This rate is 34% lower than the 'starved-sediment' case, but still in-line with results from the historically-based P&G study (-1.6 $m^3/m/yr$). Interestingly, the erosion rate decreases for subsequent higher SLRs and 'flips' to a positive sediment budget for SLR scenarios ≥1.5 m. Whereas some of this added material is due to eroded cliff material distributed across the profile between the depth of closure and the recessed cliff toe, it accounts for <30% of the total sediment added to the system. Compared to the starved-sediment system, the contributions of cliff material to the total change in the sediment budget is between 11% to 16% for all SLR scenarios up to 2 m, followed by a jump to 26% for the 5 m SLR scenario.

5. Conclusions

A profile evolution model was developed to efficiently evolve shore-normal profiles of sandy coastlines with or without cliffs along natural and urban coastal environments. The model employs the concept of dynamic equilibrium of the beach profile and translates the observed beach profile using geometry. The model is computationally efficient so that it may be applied across expansive geographic areas and at decadal to centennial time-scales in response to climate change. The model requires inputs of *a priori* calculated rates of cliff recession, lateral movement of the shoreline position (e.g., MHW), an initial profile, SLR, and the nearshore wave climate.

In this work, the profile evolution model was applied to more than 4,000 cross-shore profiles extracted from a seamless DEM of the Southern California Bight and using projected cliff recession and shoreline change results from two separate models (Limber et al. 2015; Vitousek et al. 2017) that used SLR in combination with spatial- and time-varying nearshore wave conditions. Profiles of sandy shores, cliff-backed sandy shores, and cliffed shores with narrow to no fronting beach are shown to evolve in a realistic manner. Along sandy shores, the active zone of profile translation and accumulation is taken to extend from the offshore end of the inner surf zone to a landward point defined by either a distance between the originating shoreline and vegetation, the intersection between the foreshore slope and un-eroded back-beach, or hard structures (e.g., flood protection structures). Two end-member states were considered. One state represents a sediment-starved system for which eroded cliff material was removed from the system and deposition of sediment in response to SLR, from for example overwash and aeolian transport, was not included. The second state represents ample sediment availability; this was done by distributing eroded cliff material across the profile landward of the translated cliff toe and raising the active part of the profile in response to SLR.

Total net volume changes were estimated by integrating under the evolved and original profile curves and normalizing by the alongshore distance and number of years represented by each SLR. The rates are comparable to previous work that relied on traditional sediment budget accounting methods, thus giving confidence in the results. For example, loss of sediment was projected to range from -2.9 $m^3/m/yr$ to -1.9 $m^3/yr/m$ for the 0.25 m SLR sediment-starved and ample-sediment states, respectively, an increase of ~80% and 20% compared to tallied losses based on historical records (-1.6 $m^3/m/yr$, Patch and Griggs, 2007). Comparing results of the two end-member states indicates that eroded cliff material (of yet unarmored cliffs) contribute 11% to 26% to the total sediment budget. Furthermore, modeled sediment losses associated with the 'starved-sediment' state suggest that historical (1930s through the early 1990s) beach nourishment rates will need to increase by more than 30% for a 0.25 m sea level rise and by more than 75% by the year 2100 for a sea level rise of 1 m and greater, if evolution of the shoreline is to keep pace with rising sea levels.

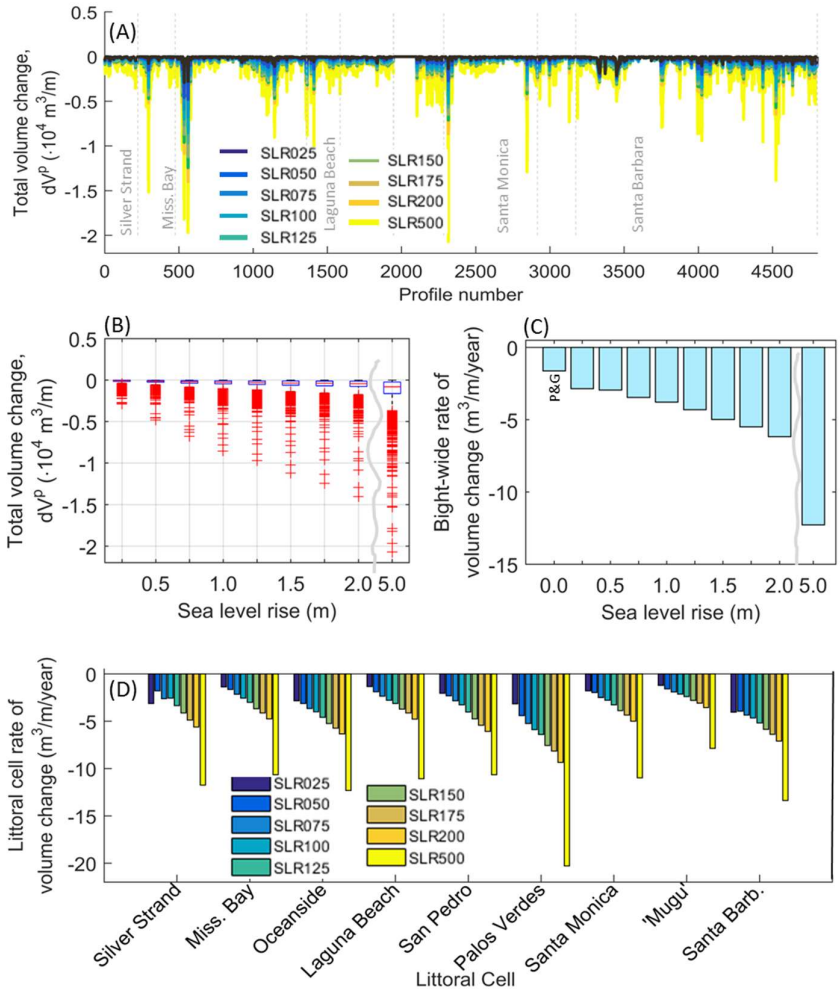

Figure 6. Projected volumetric sediment change calculated with the profile evolution algorithm seeded by *a priori* modeled cliff recession and sandy coast shoreline change rates. The cliff recession model and sandy coast shoreline change model assumes no nourishment and that erosion is limited by hard infrastructure. The profile evolution model assumes a starved sediment system with no sediment inputs. (A) Spatial variation in volumetric sediment change between evolved and initial (0 m SLR) profiles. (B) Same as in (A) but grouped by SLR and plotted as a box-plot. Central marks indicate the median, and the bottom and top edges of the boxes indicate the 25th (q_1) and 75th (q_3) percentiles, respectively. The whiskers extend to the most extreme data points not considered outliers; outliers are plotted individually using the '+' symbol, and defined as those that are greater than $q_3 + 1.5 \times (q_3 - q_1)$ or less than $q_1 - 1.5 \times (q_3 - q_1)$. (C) Bight-wide rate of volume change calculated by summing up dV^P and normalizing by the total number of years for each SLR simulated (see text for further explanation). (D) Same as in (C) but for nine littoral cells (Flick et al., 1993) within the Southern California Bight.

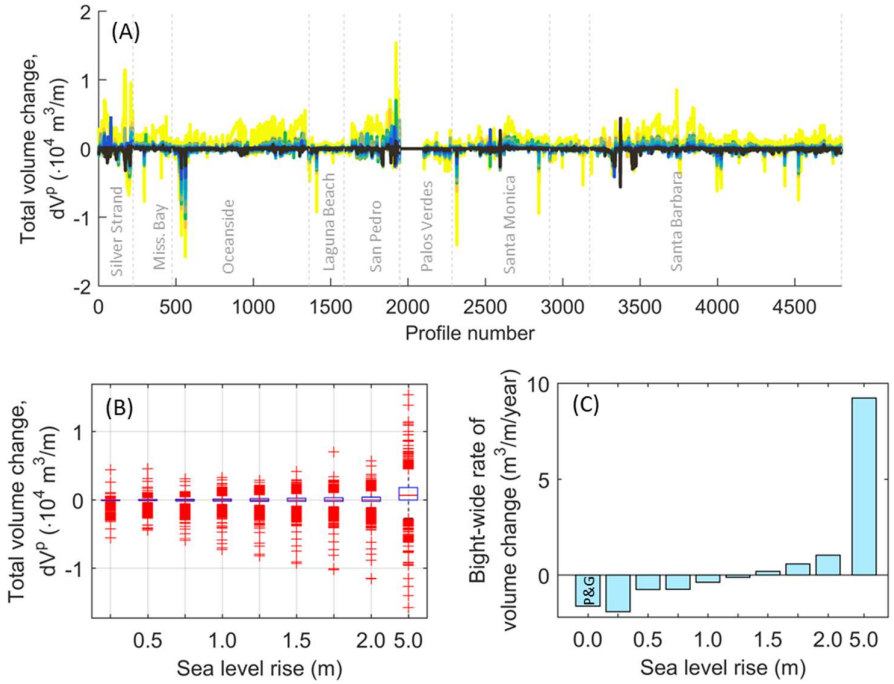

Figure 7. Same as in Figure 5 except that the profile evolution algorithm places eroded bluff material on the fronting beach and in the case of sandy shores, the elevation of the active beach is assumd to keep pace with SLR (i.e., unlimited sediment availability).

Acknowledgements

The work was completed as part of the USGS Climate Change Impacts Project, and funded in part by the California Coastal Conservancy, the USGS Mendenhall Program, and the USGS Coastal and Marine Geology Program. We thank Curst Storlazzi (USGS) and Jessica Lovering (USGS) for review of this write-up, and Dr. Lesley Ewing (California Coastal Commission) for constructive discussions. Use of trademark names does not imply USGS endorsement of products.

References

Battjes, J. A. 1974. Surf similarity. *Proceedings of the 14th Coastal Engineering Conference*, American Society of Civil Engineers, 466-480.

Bird, E., 2000. *Coastal Geomorphology: An Introduction.* John Wiley & Sons Ltd., pp. 321.

Bruun, P., 1954. *Coastal Erosion and the Development of Beach Profiles*. Beach Erosion Board Technical Memorandum 44, Washington DC: US Army Corps of Engineers, 79 pp.

Bruun, P., 1962. *Sea level rise as a cause of shore erosion*. Journal of Waterways and Harbors Division, ASCE, 88, 117–130.

Birkemeier, W.A., 1985. *Field data on seaward limit of profile change*. J. Waterways Port and Coastal Engineering, ASCE, 111, 3, 598-602,

Carter, R.W.G., 1988. *Coastal Environments. An Introduction to the Physical, Ecological and Cultural Systems of Coastlines*. Academic Press, London.

Cowell, P.J., Roy, P.S., and Jones, R.A., 1995. *Simulation of large-scale coastal change using a morphological behavior model*. Marine Geology, 126, 45-61.

Danielson, J.J., Poppenga, S.K., Brock, J.C., Evans, G.A., Tyler, D.J., Gesch, D.B., Thatcher, C.A., and Barras, J.A., 2016. *Topobathymetric elevation model development using a new methodology—Coastal National Elevation Database*. Journal of Coastal Research, SI, 76, 75–89.

Davidson-Arnott, R.G.D., 2005. *A conceptual model of the effects of sea level rise on sandy coasts*. Journal of Coastal Research, 21(6), 1166–1172.

Dean R.G., 1991. *Equilibrium beach profiles: characteristics and applications*. J. Coastal Research, 7:53–84

Fagherazzi S, Wiberg PL, Howard AD. 2003. *Tidal flow field in a small basin*. J. Geophysical Research-Oceans 108:3071–80.

FitzGerald, D.M., Fenster, M.S., Argow, B.A., and Buyenevich, I.V., 2008. *Coastal impacts due to sea-level rise*. Annual Review of Earth and Planetary Sciences, 36, 601-647.

Flick, R., 1993. *The myth and reality of Southern California beaches*, Shore Beach, 61(3), 3–13.

Hegermiller, C.A., Erikson, L.H., and Barnard, P.L., 2016, *Nearshore waves in southern California: hindcast, and modeled historical and 21st-century projected time series*. U.S. Geological Survey data release, http://dx.doi.org/10.5066/F7N29V2V

Hoover, D., 2017. *Analysis of profile data in the Santa Barbara and Ventura regions*. Personal comm.

Kaergaard, K., and Fredsoe, J., 2013. *A numerical shoreline model for shorelines with large curvature*. Coastal Engineering, 74, 19-32.

Komar, P. D., and Gaughan, M. K. 1973. *Airy wave theory and breaker height prediction*. Proceedings of the 13th Coastal Engineering Conference, American Society of Civil Engineers, 405-418.

Larson, M., and Kraus, N.C., 1989. *SBEACH: Numerical model for simulating storm-induced beach change, Report 1: Empirical foundation and model development*. TR-CERC-89-9, USACE-WES, Vicksburg, MS.

Larson, M., Westergren, S., and Hanson, H., 2015. *Modeling beach profile response to varying waves and water levels with special focus on the subaerial region*. Proceedings of Coastal Sediments 2015, World Scientific, Singapore.

Limber, P., Barnard, P., Hapke, C., 2015. *Towards projecting the retreat of California's coastal cliffs during the 21st century*. Proceedings of Coastal Sediments 2015 Conference, World Scientific, Singapore.

National Research Council (NRC), 2012. *Sea-level rise for the coasts of California, Oregon, and Washington: past, present, and future*. Committee on Sea-level rise in California, Oregon, and Washington. The National Academies Press, Washington, 260 pp.

Patch, K.B. and G.B. Griggs, 2007. *Development of sand budgets for California's major littoral cells*. UC Santa Cruz, California Dept. of Boating and Waterways, California Sediment Management Work Group. 115pp.

Pilkey, O.H., Young, R.S., Riggs, S.R., Smith, S., Wu, H., and Pilkey, W.D., 1993. *The concept of shoreface profile equilibrium: a critical review*. J. Coastal Research 9:255–78.

Ranasinghe, R., and Stive, M. J., 2009. *Rising seas and retreating coastlines*. Climatic Change, 97(3), 465-468.

Raubenheimer, B., and Guza, R.T., 1996. *Wave transformation across the inner surf zone*. J. Geophysical Research, 101, C10, 25,589-25,597.

Roelvink, J. A., and Van Banning, G. K. F. M., 1995. *Design and development of DELFT3D and application to coastal morphodynamics*. Oceanographic Literature Review, 11(42), 925.

Roelvink, D., Reniers, A. J. H. M., Van Dongeren, A., Van Thiel de Vries, J., Lescinski, J., and McCall, R., 2010. *XBeach model description and manual*. Unesco-IHE Institute for Water Education, Deltares and Delft University of Tecnhology. Report.

Rosati, J.D. Dean, R.G., and Walton, T.L., 2013. *The modified Bruun Rule extended for landward transport*. Marine Geology, 340, 71-81.

Stive, M.J.F., Aarninkhof, S.G.J., Hamm, L., Hanson, H., Larson, M., Wijnberg, K.M., Nicholls, R.J., and Capobianco, M., 2002. *Variability of shore and shoreline evolution*. Coastal Engineering, 47, 211-235.

Thatcher, C.A., Brock, J.C., Danielson, J.J., Poppenga, S.K., Gesch, D.B., Palaseanu-Lovejoy, M.E., Barras, J.A., Evans, G.A., and Gibbs, A.E., 2016. *Creating a Coastal National Elevation Database (CoNED) for science and conservation applications*. Journal of Coastal Research, SI, 76, 64–74.

Trenhaile, A.S., 2011. *Predicting the response of hard and soft rock coasts to changes in sea level and wave height*. Climatic Change, 109:599-615.

Vitousek, S., Barnard, P.L, Limber, P., Erikson, L., Cole, B., 2017. *A model integrating longshore and cross-shore processes for predicting long-term shoreline response to climate change*. J. Geophysical Research Earth Surface, 122, 25pp.

Warner, J. C., Armstrong, B., He, R., and Zambon, J. B., 2010. *Development of a coupled ocean–atmosphere–wave–sediment transport (COAWST) modeling system*. Ocean modelling, 35(3), 230-244.

Warren, I. R., and Bach, H., 1992. *MIKE 21: a modelling system for estuaries, coastal waters and seas*. Environmental Software, 7(4), 229-240.

Walkden M.J.A., and Hall, J.W., 2005. *A predictive mesoscale model of the erosion and profile development of soft rock shores*. Coastal Engineering, 52, 55-563.

Young, A.P., Flick, R.E., O'Reilly, W.C., Chadwick, D.B., Crampton, W.C. and Helly, J.J., 2014. *Estimating cliff retreat in southern California considering sea level rise using a sand balance approach*. Marine Geology, 348, 15-26.